Int J Clin Exp Pathol 2020;13(4):685-691
www.ijcep.com /ISSN:1936-2625/IJCEP0089668

Original Article

miR-566 expression and immune changes in patients with intracranial aneurysm

Hongjun Fan, Chun Yang, Chenguang Jia, Xingyun Xie, Li Du

Department of Neurosurgery, Zhuzhou Central Hospital, Zhuzhou, Hunan, China

Received December 11, 2018; Accepted January 15, 2019; Epub April 1, 2020; Published April 15, 2020

Abstract: Objective: Our study aims to investigate the correlations of micro ribonucleic acid (miR)-566 expression with the changes in immune-related indexes and differential genes in patients with intracranial aneurysm (IA). Methods: Aneurysm wall tissues from a total of 50 IA cases and the corresponding normal arterial wall tissues from 50 individuals were selected. The miR-566 expression, differential gene expression profile, and expression level of differential gene proteins were detected and analyzed by fluorescence quantitative polymerase chain reaction (qPCR), RNAseq technique and western blotting, respectively. Results: The miR-566 level was significantly higher in intracranial aneurysm tissues than that in normal arterial wall tissues ($P<0.05$). The levels of cluster of differentiation (CD)3^+, $CD4^+$, $CD8^+$, $CD4^+/CD8^+$ and $CD23^+$ T lymphocytes in the peripheral blood of IA patients significantly declined compared with those in the control group ($P<0.05$). RNAseq detection showed that there were 16 immune-inflammation-related genes significantly differentially expressed in aneurysm wall tissues compared with normal arterial wall tissues in the control group. The levels of VHL and NIK in aneurysm wall tissues were significantly decreased, while those of VEGF and ALOX5 were obviously increased. Both mRNA and protein levels of these four genes also had significant changes, which had linear relations to the expression of miR-566. Conclusion: The abnormal expression of miR-566 affects the immune function, thus promoting the occurrence and deterioration of intracranial aneurysm.

Keywords: Intracranial aneurysm, miR-566, immune, genetic screening

Introduction

Intracranial aneurysm (IA) is a kind of tumor-like lesion induced by the abnormal swelling in the intracranial arterial wall [1]. Rupture is the leading cause of subarachnoid hemorrhage, accounting for 70-90% of the total cases. IA contributes to critical cerebrovascular accidents besides cerebral infarction and hypertensive cerebral hemorrhage, which can occur at any age, but mostly at the age of 40-60 years [2]. In terms of clinical manifestations, both mortality and disability rates are extremely high. The pathogenesis of IA remains unclear while the results in clinical screening still need to be further improved. At the same time, there are no effective therapeutics and intervention means in its clinical practice [3].

The formation, development and rupture of IA have close correlations with the immuno-inflammatory responses in the body. It has been confirmed that, in the perioperative period, the inflammatory response regulated by cytokines in patients with IA is significantly enhanced, which breaks the immune homeostasis and affects the postoperative recovery rate [4]. The massive secretion of tumor necrosis factor (TNF) [5] and interleukin-4 (IL-4) are induced [6-8], and has a significant linear relation with the malignant grade of IA.

Micro ribonucleic acid (miRNA), as a kind of non-coding single-stranded RNA molecule, involved in the regulation of post-transcriptional gene expression in the pathophysiologic process, plays an important role in carcinogenic pathway and immune response [9-11]. It is reported that the abnormal expression of miRNA may lead to the imbalance of regulation of oncogenes or tumor suppressor genes, thus affecting the occurrence and development of tumor [12]. In addition, miRNAs can also serve as biomarkers for the diagnosis and prognosis

Table 1. Primer sequences of qPCR

Primer	Sequence
miR-566-F	ATGGTTCGTGGGATACACATACACGCA
miR-566-R	GCAGGGTCCGAGGTATTC
U6-F	GCTTCGGCAGCACATATACTAAAAT
U6-R	CGCTTCACGAATTTGCGTGTCAT
VHL-F	GGAGCCTAGTCAAGCCTGAGA
VHL-R	CATCCGTTGATGTGCAATGCG
NIK-F	CATTGGCCTTGGTACTTATGGC
NIK-R	GTCTTACGAGCGTTCATCACTT
VEGF-F	GAGGAGCAGTTACGGTCTGTG
VEGF-R	TCCTTTCCTTAGCTGACACTTGT
ALOX5-F	TCAGCGTGGTCCAGAATGG
ALOX5-R	GCAAGTGTTCCGGTCCTCT
β-actin-F	AAGGAGCCCCACGAGAAAAAT
β-actin-R	ACCGAACTTGCATTGATTCCAG

of tumor, and even potential targets for the determination of tumor grade and anti-cancer treatment. Previous evidence indicated that miR-338-3p, miR-200a [13], and miR-566 are abnormally expressed in a variety of tumors, such as glioblastoma [14-17], colon cancer [18] and lung adenocarcinoma [19]. However, neither expression nor function of miR-566 in IA is clear. In this study, therefore, we aimed to explore the expression of miR-566 in aneurysm specimens of patients with IA and determine its role in the immuno-inflammatory regulation.

Materials and methods

Materials

In this study, 50 patients with IA in Zhuzhou Central Hospital from May 2016 to May 2018 were selected as the experimental group, including 26 males (52%) and 24 females (48%) with an average age of (44.6±10.90) years. Another 50 healthy subjects receiving physical examination in Zhuzhou Central Hospital from December 2017 to August 2018 were selected as control group, including 18 males (36%) and 32 females (74%) with an average age of (41±16.87) years. Patients and their family members agreed and signed the informed consent about the experimental sampling, and this experiment was reviewed by the Ethics Committee of hospital.

TRIzol kit (Tiangen), miRNA Isolation kit (Ambion), RNeasy Mini Elute Taqman microRNA detection kit (TAKARA): TaqMan microRNA reverse transcription kit (TAKARA), Fragmentation Buffer (TAKARA), and Quick polymerase chain reaction (PCR) kit (TAKARA).

$CD3^+$, $CD4^+$, $CD8^+$, $CD4^+/CD8^+$, $CD23^+$, von Hippel-Lindau (VHL), vascular endothelial growth factor (VEGF), NF-κB-inducing kinase (NIK), arachidonate 5-lipoxygenase (ALOX5) and β-actin antibodies were from Santa Cruz. Red blood cell lysis buffer was purchased from Beyotime.

The primers used were synthesized by Shanghai Sunny Biotechnology Co., Ltd. (**Table 1**).

Real-time quantitative PCR (RT-qPCR): The total RNA was extracted from samples using the miRNA Isolation kit according to the instructions as follows: Tissues were ground into powder in a grinder first, and then placed in the miRNA Isolation reagent, followed by homogenization using a homogenizer. After chloroform was added, the mixture was centrifuged using a refrigerated centrifuge. The RNA was then collected from the upper colorless and transparent layer. It was dissolved in RNase-free water and transferred to the RNeasy MinElute filter column for centrifugation. Finally, the pure total RNA was obtained. RNA was reversely transcribed to obtain the reverse transcription product using the TaqMan microRNA reverse transcription kit according to the instructions, followed by detection on the fluorescence qPCR instrument (ABI7500). Then the data were exported and analyzed. The relative expression level of miR-566 was analyzed using the $2^{-\Delta\Delta Ct}$ method. $\Delta\Delta Ct$ = [aneurysm ($Ct^{miR\text{-}566}$ - Ct^{U6})] - [normal control tissues ($Ct^{miR\text{-}566}$ - Ct^{U6})].

Immunoassay

In IA group, 2 mL fasting peripheral blood was collected before operation to detect T lymphocyte levels. In control group, 2 mL peripheral blood was collected on the day of physical examination. T lymphocyte contents ($CD3^+$, $CD4^+$, $CD8^+$, $CD4^+/CD8^+$ and $CD23^+$) were detected by flow cytometry.

RNAseq analysis

Total RNA extraction and library construction: The total RNA was extracted from tissue samples according to instructions of the TRIzol kit, and dissolved in RNase-free water. The concentration of RNA was determined, and the purity

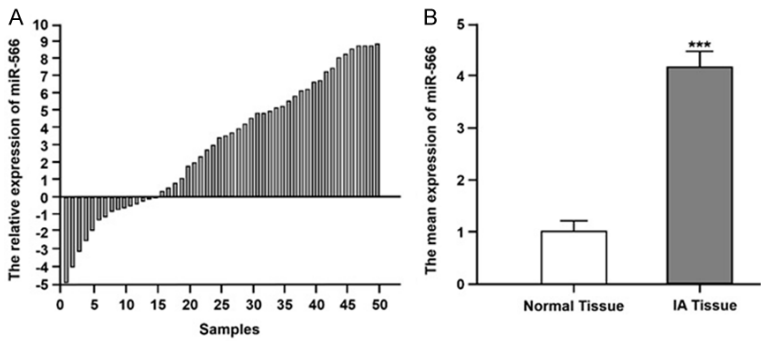

Figure 1. Expression of miR-566 in aneurysm wall tissues and normal control arterial wall tissues. A: Relative expression of miR-566 in 50 pairs of tissues, B: Mean expression of miR-566 in 50 pairs of tissues (***P=0.0008).

of RNA and whether there was degradation were detected by gel electrophoresis. Then messenger RNA (mRNA) was enriched using oligosaccharide magnetic beads, and rRNA was removed using the TAKARA kit. The fragment buffer was added into the mRNA fragment, and the first strand and two strands of complementary deoxyribonucleic acid (cDNA) were synthesized using six base random primers, followed by purification and elution using the quick PCR kit. After that, the sequencing joint was applied, the target fragment was amplified via agarose gel electrophoresis, and a complete library was constructed. The library constructed was sequenced using Illumina HISEQ2000.

RNAseq data processing

After library construction and sequencing, the intensity and ratio of signal were analyzed using the DESeq21.14.1 software. The data in each library were standardized, and then the gene probe numbers with differential expression in the two kinds of tissues were screened. The corresponding gene and biological information were inquired on the NCBI (www.ncbi.nlm.nih.gov).

Western blotting analysis

The aneurysm wall tissues and normal control arterial wall tissues were homogenized with 1 mL 0.1% SDS-Trition-X00 tissue lysis buffer. After there were no visible tissues to the naked eye, centrifugation was performed at 12,000 rpm and 4°C for 10 min. The supernatant was collected as the total protein sample. The protein was quantified using the bicinchoninic acid protein quantitative kit (Millipore), and the total protein concentration in cortical tissues in each group was calculated. The sample loading system in an equal concentration was prepared, and heated at 95°C for 15 min to inactivate the protein. Then the sample was added into the sodium dodecyl sulfate polyacrylamide gel electrophoresis (SDS-PAGE) gel slot prepared for electrophoresis until the protein completely reached the bottom of the gel. The protein was transferred onto a polyvinylidene fluoride membrane (Millipore) under constant current of 260 mA. The membrane was sealed with the freshly-prepared 5% skim milk powder for 2 h, and the target band was cut according to the protein size. The band was incubated with primary antibodies overnight, washed with tris-buffered saline with Tween-20 (TBST) for 3 times (10 min per time), incubated with horseradish peroxidase-conjugated secondary antibody (Millipore) at room temperature for 2 h, and washed again with TBST for 3 times (10 min per time). Finally, enhanced chemiluminescence solution (Millipore) was added for color development using a developing machine to calculate the relative expression level of the corresponding protein.

Statistical methods

SPSS software was used for the statistical analysis of all data. *t* test statistical method was used for the intergroup comparison of data. Chi-square test was adopted for the analysis of enumeration data. Measurement data were expressed as mean ± standard deviation ($\bar{x}\pm s$). *P*-values <0.05 were considered significant.

Results

Expression level of miR-566 in IA tissues

To investigate the clinical correlation between miR-566 and IA, the expression of miR-566 from 50 pairs of IA tissues and normal tissues was detected by RT-qPCR (**Figure 1A**). The result indicated that miR-566 was up-regulated in 37 IA tissues. The mean expression of miR-566 is shown in **Figure 1B**, and it can be seen that the level of miR-566 in IA tissues was significantly higher than that in normal tissues (P<0.001).

Table 2. T lymphocyte levels in IA patients, comparisons of $CD3^+$, $CD4^+$, $CD8^+$, $CD4^+/CD8^+$ and $CD23^+$ T lymphocyte levels ($\overline{X}\pm s$)

Group	n	$CD3^+$	$CD4^+$	$CD8^+$	$CD4^+/CD8^+$	$CD23^+$
IA group	50	55.3±5.3	33.2±7.9	29.3±1.9	1.1±0.3	38.2±2.2
Control group	50	68.3±2.1*	45.3±1.7*	37.3±0.3*	1.2±0.3*	42.9±5.2*
F		59.239	38.317	4.311	22.562	40.890

Note: *$P<0.05$ in control group vs. IA group.

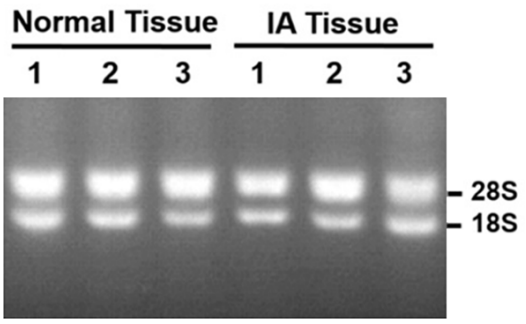

Figure 2. Extraction and detection of total RNA.

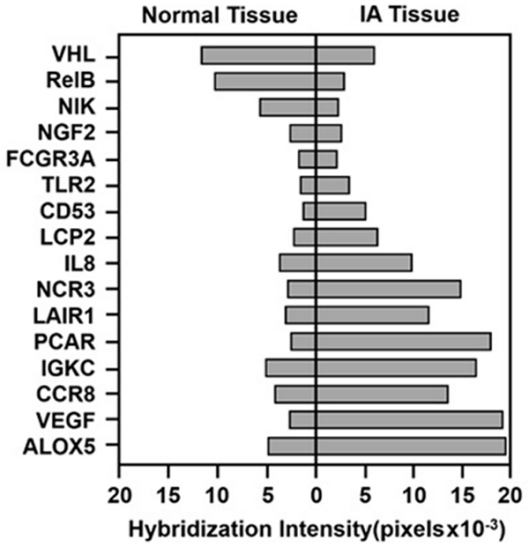

Figure 3. Differential gene expression between IA and normal groups.

T lymphocyte levels in IA patients

$CD3^+$, $CD4^+$, $CD8^+$, $CD4^+/CD8^+$ and $CD23^+$ T lymphocyte levels were detected by flow cytometry, and the contents in the peripheral blood were compared before and after operation in the IA group. Results revealed that there were statistically significant differences in $CD3^+$ [(55.3±5.3)%], $CD4^+$ [(33.2±7.9)%], $CD8^+$ [(29.3±1.9)%], $CD4^+/CD8^+$ [(1.1±0.3)] and $CD23^+$ [(38.2±2.2)%] in IA group compared with those in control group ($P<0.05$) (**Table 2**), indicating that the autoimmunity of IA patients was suppressed.

Extraction of total RNA from IA tissues and normal tissues

As shown in **Figure 2**, both 28S and 18S, as measurement indexes for RNA integrity, were evidently observed, suggesting no dramatic degradation of RNA. The above results lay a foundation for the detection of differential gene expression profiles in IA tissues and normal tissues using RNAseq technique.

Differential gene expression in IA detected by RNAseq technique

It was found that about 256 genes were differently expressed in IA patients compared with normal individuals. Of note, the levels of 4 genes were significantly decreased, while those of 12 genes were obviously increased **Figure 3**.

mRNA expressions of immune-related controlling genes in IA detected by qPCR

The mRNA expressions of immune-related controlling genes (VHL, VEGF, NIK and ALOX5) in IA tissues and normal tissues were detected by qPCR. As shown in **Figure 4**, the levels of VHL and NIK genes in IA tissues were significantly decreased compared with those in normal tissues, while those of VEGF and ALOX5 genes in IA tissues were obviously increased, which were consistent with the RNAseq results.

Protein expressions of immune-related controlling genes in IA detected by western blotting

The protein expression levels of immune-related controlling genes (VHL, VEGF, NIK and ALOX5) in IA tissues and normal tissues were

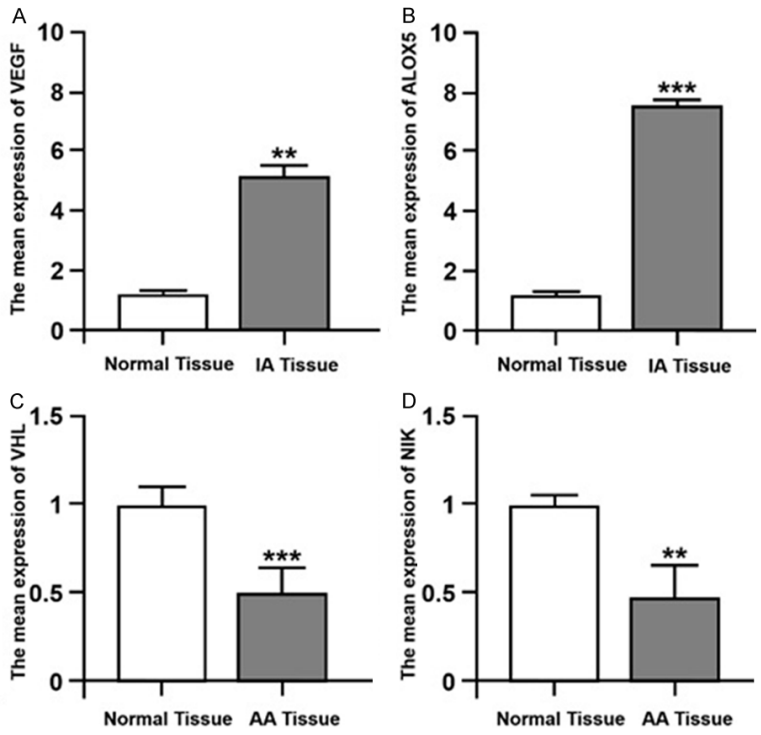

Figure 4. mRNA relative expression of immune-related controlling genes detected by qPCR: VEGF (A, $^{**}P$=0.0085), ALOX5 (B, $^{***}P$=0.00075), VHL (C, $^{***}P$=0.0091) and NIK (D, $^{**}P$=0.0097).

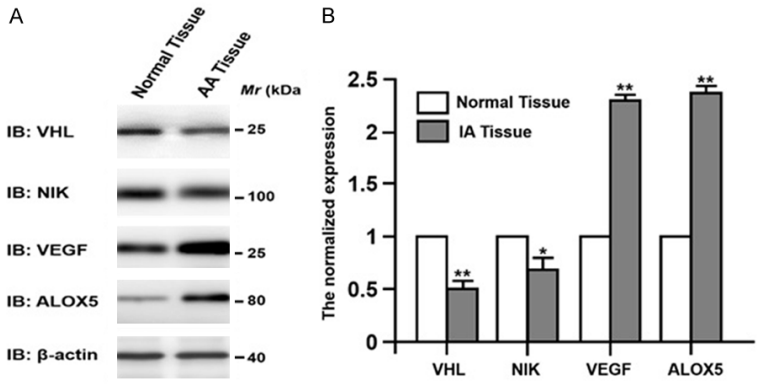

Figure 5. Protein expression of immune-related controlling genes detected byt western blotting. A: VHL, NIK, VEGF and ALOX5 expression in IA detected by western blotting, B: Statistical results of VHL, NIK, VEGF and ALOX5 expression in IA (VHL: $^{**}P$=0.0073, NIK: $^{*}P$=0.0030, VEGF: $^{**}P$=0.0053, ALOX5: $^{**}P$=0.00449).

detected by western blotting. Similarly, as shown in **Figure 5A** and **5B**, the levels of VHL and NIK proteins in IA tissues were significantly decreased compared with those in normal tissues, while those of VEGF and ALOX5 genes in IA tissues were obviously increased.

Linear relations of miR-566 expression level with VHL, VEGF, NIK and ALOX5 gene expressions

The linear relations of miR-566 expression level with VHL, VEGF, NIK and ALOX5 gene expression levels in 50 pairs of IA tissues and normal tissues were compared, and it was found that the miR-566 expression level had linear relations with VHL, VEGF, NIK and ALOX5 gene expressions. Notably, the increase of miR-566 expression level reduced VHL and NIK gene expressions, while elevated VEGF and ALOX5 gene expressions (**Figure 6**).

Discussion

IA rupture hemorrhage is one of the most common causes of subarachnoid hemorrhage in clinic, leading to severe disability and death of patients [1]. Therefore, the diagnosis and treatment of IA has become an important part in the study on IA. It has been found in studies that the precipitating factors of IA are very complicated [2], among which, smoking, excessive drinking and obesity are closely related to the development of IA [1]. In addition, cocaine was reported to result in the formation and rupture of IA [5]. Several genetic diseases can also increase the prevalence rate of aneurysm, such as autosomal dominant polycystic kidney disease and neurofibromatosis. 10-15% patients with autosomal dominant polycystic kidney disease suffer from IA lesions [8].

Previous study has unraveled the differential miRNA expression in IA wall and autologous normal arterial wall specimens by using the

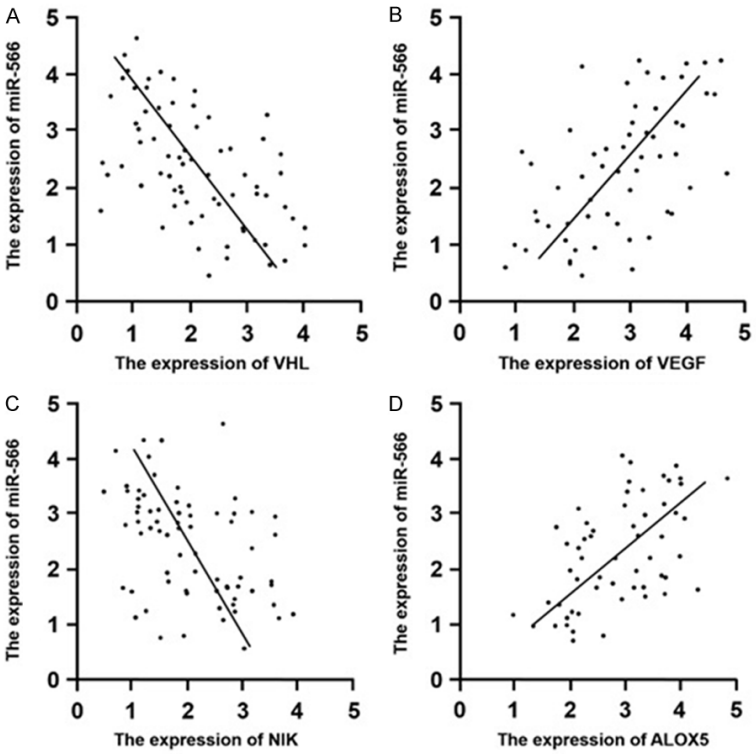

Figure 6. Linear analysis of miR-566 expression level with VHL (A: r=0.81, P=6.7^{e9}), VEGF (B: r=0.77, P=8.3^{-e8}), NIK (C: r=0.89, P=9.3^{e8}) and ALOX5 (D: r=0.63, P=8.2^{-e7}) gene expression.

miRNA array, and it indicated that significant differences were found among miR-566, miR-99b and miR-1180 expressions, in which miR-566 has a significant correlation with immuno-inflammatory responses [10]. Our data by using the RNAseq technique unraveled that among 256 differential genes of IA patients, the expression levels of 4 genes were significantly decreased, while those of 12 genes were obviously increased in comparison to normal control. The occurrence and rupture of IA are also closely related to the immune response in patients. For instance, pro-inflammatory cytokines are highly expressed in the IA wall [7], and their levels and activation degree showed linear relations with the risk level of IA. In microarray analysis, the result manifested that there were differential expressions in complement-related genes in IA compared with control arterial wall specimens, and immunohistochemical results showed that complement components C3 and C9 were activated in most unruptured IA. Also, IgG and IgM related to IA were also activated [8]. In terms of immune-induced cell inflammatory response, there is often excessive recruitment and exosmosis of leukocytes in IA, suggesting that the endothelium is being activated and inflammatory infiltration is produced in IA and its adjacent tissues [20]. In this study, the expression level of miR-566 was detected in 50 patients with IA, and we found that miR-566 was highly expressed in 70% patients. The expression of miR-566 in IA was significantly increased compared to that in autologous control vessel specimens (normal artery). We observed that the levels of $CD3^+$, $CD4^+$, $CD8^+$, $CD4^+/CD8^+$ and $CD23^+$ T lymphocytes in the peripheral blood of IA group present statistically significant differences compared with those in the control group, suggesting that the autoimmunity of IA patients was impeded. It has been demonstrated that the important molecule DAMP involved in the activation of macrophages and T lymphocytes (through dendritic cells) may participate in the formation of IA [19]. These data imply the correlation between miRNA expression and immune-inflammation-related genes in IA has important scientific and clinical research values.

Furthermore, previous evidence exhibited that miR-566 can regulate the expression of VHL, indicating that there are correlations among the high expression of miR-566, low levels of T lymphocytes and disorders of immune gene expression in IA patients. The inhibition of miR-566 expression can increase the VHL expression and reduce the VEGF expression, thereby inhibiting migration and infiltration of tumor cells [16, 17]. Consistently, we found that as the miR-566 expression was increased, levels of VHL and NIK were markedly declined, while VEGF and ALOX5 were markedly elevated, indicating the involvement of miR-566 in the imbalance of immune-inflammation homeostasis occurs in IA patients.

Conclusion

Our data demonstrate that the level of miR-566 is remarkably increased in patients with intra-

cranial aneurysm. miR-566 is associated with the attenuation of immuno-inflammatory response in IA patients, which provides new ideas for the further development of anti-inflammatory drugs in the treatment of IA formation and rupture.

Acknowledgements

This work was supported by the Health and Family Planning Commission Research Fund of Hunan Province (B2015-160); the Science and Technology Department Fund of Zhuzhou City (2018-126).

Disclosure of conflict of interest

None.

Address correspondence to: Dr. Hongjun Fan, Department of Neurosurgery, Zhuzhou Central Hospital, 116 South of Changjiang Road, Tianyuan District, Zhuzhou 412000, Hunan, China. Tel: +86-731-28219219; Fax: +86-731-28219219; E-mail: hongjunfan7wn@163.com

References

[1] Ohkuma H, Suzuki S, Fujita S and Nakamura W. Role of a decreased expression of the local renin-angiotensin system in the etiology of cerebral aneurysms. Circulation 2003; 108: 785-787.

[2] Rutka JT, Taylor M, Mainprize T, Langlois A, Ivanchuk S, Mondal S and Dirks P. Molecular biology and neurosurgery in the third millennium. Neurosurgery 2000; 46: 1034-1051.

[3] Du P, Kibbe WA and Lin SM. Lumi: a pipeline for processing illumina microarray. Bioinformatics 2008; 24: 1547-1548.

[4] Chyatte D, Bruno G, Desai S and Todor DR. Inflammation and intracranial aneurysms. Neurosurgery 1999; 45: 1137-1146; discussion 1146-1137.

[5] Jayaraman T, Berenstein V, Li X, Mayer J, Silane M, Shin YS, Niimi Y, Kilic T, Gunel M and Berenstein A. Tumor necrosis factor-α is a key modulator of inflammation in cerebral aneurysms. Neurosurgery 2005; 57: 558-564.

[6] Ostergaard JR, Kristensen BO, Svehag SE, Teisner B and Miletic T. Immune complexes and complement activation following rupture of intracranial saccular aneurysms. J Neurosurg 1987; 66: 891-897.

[7] Shimizu K, Mitchell RN and Libby P. Inflammation and cellular immune responses in abdominal aortic aneurysms. Arterioscler Thromb Vasc Biol 2006; 26: 987-94.

[8] Pan JH, Lindholt JS, Sukhova GK, Baugh JA, Henneberg EW, Bucala R, Donnelly SC, Libby P, Metz C and Shi GP. Macrophage migration inhibitory factor is associated with aneurysmal expansion. J Vasc Surg 2003; 37: 628-635.

[9] Catto JW, Alcaraz A, Bjartell AS, De Vere White R, Evans CP, Fussel S, Hamdy FC, Kallioniemi O, Mengual L, Schlomm T and Visakorpi T. MicroRNA inprostate, bladder, and kidney cancer: a systematic review. Eur Urol 2011; 59: 671-681.

[10] Su X, Xing J, Wang Z, Chen L, Cui M and Jiang B. microRNAs and ceRNAs: RNA networks in pathogenesis of cancer. Chin J Cancer Res 2013; 25: 235-239.

[11] Homami A and Ghazi F. MicroRNAs as biomarkers associated with bladder cancer. Med J Islam Repub Iran 2016; 30: 475.

[12] Enokida H, Yoshino H, Matsushita R and Nakagawa M. The role of microRNAs in bladder cancer. Invest Clin Urol 2016; 57 Suppl 1: S60-76.

[13] Fu H, Song W, Chen X, Guo T, Duan B, Wang X, Tang Y, Huang L and Zhang C. MiRNA-200a induce cell apoptosis in renal cell carcinoma by directly targeting SIRT1. Mol Cell Biochem 2018; 437: 143-152.

[14] Zhang X, Wang C, Li H, Niu X, Liu X, Pei D, Guo X, Xu X and Li Y. miR-338-3p inhibits the invasion of renal cell carcinoma by downregulation of ALK5. Oncotarget 2017; 8: 64106-64113.

[15] Xiao B, Zhou X, Ye M, Lv S, Wu M, Liao C, Han L, Kang C and Zhu X. MicroRNA-566 modulates vascular endothelial growth factor by targeting Von Hippel-Landau in human glioblastoma in vitro and in vivo. Mol Med Rep 2016; 13: 379-385.

[16] Wagner EJ, Li M and Kang CS. MicroRNA-566 activates EGFR signaling and its inhibition sensitizes glioblastoma cells to nimotuzumab. Mol Cancer 2014; 13: 63.

[17] Jayaraman T, Paget A, Shin YS, Li X, Mayer J, Chaudhry H, Niimi Y, Silane M and Berenstein A. TNF-alpha-mediated inflammation in cerebral aneurysms: a potential link to growth and rupture. Vasc Health Risk Manag 2008; 4: 805-817.

[18] Drusco A, Nuovo GJ, Zanesi N, Di Leva G, Pichiorri F, Volinia S, Fernandez C, Antenucci A, Costinean S, Bottoni A, Rosito IA, Liu CG, Burch A, Acunzo M, Pekarsky Y, Alder H, Ciardi A and Croce CM. MicroRNA profiles discriminate among colon cancer metastasis. PLoS One 2014; 9: e96670.

[19] Rani S, Gately K, Crown J, O'Byrne K and O'Driscoll L. Global analysis of serum microRNAs as potential biomarkers for lung adenocarcinoma. Cancer Biol Ther 2013; 14: 1104-1112.

[20] Peters DG, Kassam AB, Feingold E, Heidrich-O'Hare E, Yonas H, Ferrell RE and Brufsky A. Molecular anatomy of an intracranial aneurysm: coordinated expression of genes involved in wound healing and tissue remodeling. Stroke 2001; 32: 1036-1042.